



A New Negative Allosteric Modulator AP14145 for the Study of Small Conductance Calcium-Activated Potassium Channels

Simo Vicens, Rafel; Kirchhoff, Jeppe Egedal; Dolce , Bernardo ; Abildgaard, Lea; Speerschneider, Tobias; Sørensen, Ulrik Svane; Grunnet, Morten; Diness, Jonas Goldin; Bentzen, Bo Hjorth

Published in:
British Journal of Pharmacology

DOI:
[10.1111/bph.14043](https://doi.org/10.1111/bph.14043)

Publication date:
2017

Document version
Peer reviewed version

Citation for published version (APA):
Simo Vicens, R., Kirchhoff, J. E., Dolce , B., Abildgaard, L., Speerschneider, T., Sørensen, U. S., ... Bentzen, B. H. (2017). A New Negative Allosteric Modulator AP14145 for the Study of Small Conductance Calcium-Activated Potassium Channels. *British Journal of Pharmacology*, 174(23), 4396-4408. <https://doi.org/10.1111/bph.14043>

1 **A New Negative Allosteric Modulator AP14145 for the Study of Small**
2 **Conductance Calcium-Activated Potassium Channels**

3 **Running title: Novel K_{Ca}2 Channel Inhibitor**

4 Rafel Simó-Vicens^{1,2}, Jeppe E. Kirchhoff², Bernardo Dolce³, Lea Abildgaard Jensen²,
5 Tobias Speerschneider², Ulrik S. Sørensen², Morten Grønnet², Jonas G. Diness², Bo H.
6 Bentzen^{1,2}

7 *¹Biomedical Institute, University of Copenhagen, Blegdamsvej 3B, DK-2200,*
8 *Copenhagen, Denmark*

9 *²Acesion Pharma, Ole Maaløes Vej 3, DK-2200, Copenhagen, Denmark.*

10 *³Department of Experimental Pharmacology and Toxicology, University Medical*
11 *Center Hamburg-Eppendorf, Germany & DZHK (German Center for Cardiovascular*
12 *Research), partner site Hamburg/Kiel/Lübeck, Hamburg*

13

14

15 Corresponding author: Bo H. Bentzen, bobe@sund.ku.dk, Blegdamsvej 3B, DK-2200,
16 Copenhagen, Denmark

17

18 **Abbreviations:**

19 AERP: atrial effective refractory period

20 AF: atrial fibrillation

21 K_{Ca}1.1 big conductance calcium-activated potassium channel

22 K_{Ca}2: small conductance calcium-activated potassium channel

23 K_{Ca}3.1: intermediate conductance calcium-activated potassium channel

24 PEG: polyethylene glycol

25 WT: wild type

26

27

28

29 **Abstract**

30 **Background and purpose:** Small conductance Ca^{2+} -activated K^+ ($\text{K}_{\text{Ca}2}$) channels
31 represent a promising atrial-selective target for treatment of atrial fibrillation (AF).
32 Here, we establish the mechanism of $\text{K}_{\text{Ca}2}$ inhibition by the new compound AP14145.

33 **Experimental approach:** Using site directed mutagenesis binding determinants for
34 AP14145 inhibition were explored. AP14145 selectivity and mechanism of action were
35 investigated by patch clamp recordings of heterologously expressed $\text{K}_{\text{Ca}2}$ channels. The
36 biological efficacy of AP14145 was assessed by measuring atrial effective refractory
37 period (AERP) prolongation in anaesthetised rats and a beam walk test was performed
38 in mice to determine acute CNS related effects of the drug.

39 **Key results:** AP14145 was found to be an equipotent negative allosteric modulator of
40 $\text{K}_{\text{Ca}2.2}$ and $\text{K}_{\text{Ca}2.3}$ channels ($\text{IC}_{50} = 1.1 \pm 0.3 \mu\text{M L}^{-1}$). The presence of AP14145 (10
41 $\mu\text{M L}^{-1}$) increased the EC_{50} of Ca^{2+} on $\text{K}_{\text{Ca}2.3}$ from $0.36 \pm 0.02 \mu\text{M L}^{-1}$ to $1.2 \pm 0.1 \mu\text{M}$
42 L^{-1} . The inhibitory effect strongly depended on two amino acids, S508 and A533.
43 AP14145 concentration-dependently prolonged AERP in rats. Moreover, AP14145 (10
44 mg kg^{-1}) did not trigger any apparent CNS effects in mice.

45 **Conclusion and implications:** AP14145 is a negative allosteric modulator of $\text{K}_{\text{Ca}2.2}$
46 and $\text{K}_{\text{Ca}2.3}$ that shifts the calcium dependence of channel activation, an effect strongly
47 dependent on two identified amino acids. AP14145 prolongs AERP in rats and does not
48 trigger any acute CNS effects in mice. The understanding of how $\text{K}_{\text{Ca}2}$ inhibition is
49 accomplished at the molecular level will help future development of drugs targeting
50 $\text{K}_{\text{Ca}2}$ channels.

51

52

53

54

55

56

57

58 **Introduction**

59 Small conductance calcium-activated potassium channels ([K_{Ca}2.1](#), [K_{Ca}2.2](#) and [K_{Ca}2.3](#)
60 channels) are widely distributed in humans (Chen et al., 2004), where they serve
61 important roles such as contributing to the afterhyperpolarization in neurons (Pedarzani
62 et al., 2005), the endothelium-derived hyperpolarization (Milkau et al., 2010) or the late
63 repolarization phase in cardiomyocytes (Li et al., 2009). These channels are
64 constitutively associated to calmodulin, which binds intracellular calcium and activates
65 K_{Ca}2 (Adelman, 2016). Since cloning of the channels 20 years ago (Köhler et al., 1996),
66 they have piqued the interest of pharmacologists in different therapeutic areas. Although
67 at the beginning most of the efforts were focused on the CNS and the treatment of
68 neurodegenerative and psychiatric diseases (Lam et al., 2013), the therapeutic potential
69 of K_{Ca}2 channels rapidly spread to other areas (Wulff et al., 2007). Currently, one of the
70 most promising therapeutic opportunities for K_{Ca}2 channel modulation seems to be in
71 cardiovascular diseases, more specifically in atrial fibrillation (AF).

72 AF is the most common type of cardiac arrhythmia and it is considered one of the
73 largest public health problems in developed countries (Zoni-Berisso et al., 2014). The
74 disease is characterized by rapid uncoordinated activation of the atria, resulting in
75 reduced ventricular filling and blood stasis in atria, which predisposes to heart failure
76 and thromboembolic stroke (Nattel, 2002). Unfortunately, current rhythm therapy is
77 only moderately effective and may trigger serious non cardiac as well as ventricular
78 adverse effects (Waks and Zimetbaum, 2017).

79 K_{Ca}2 channels are considered a promising new target for AF treatment for several
80 reasons. First, the functional role of K_{Ca}2.2 and K_{Ca}2.3 channels appears to be greater in
81 the atria as compared to ventricles which may help avoiding undesired ventricular
82 adverse effects (Diness et al., 2015). Second, K_{Ca}2 channel inhibition prolongs the atrial
83 effective refractory period (AERP, Diness *et al.*, 2010), a pharmacological strategy that
84 has successfully been used in the development of other class III antiarrhythmic drugs
85 (Schmitt et al., 2014). Furthermore, common variants of the genes that encode K_{Ca}2.2
86 and K_{Ca}2.3 have been associated with atrial fibrillation (Ellinor et al., 2010;
87 Christophersen et al., 2017).

88 The first described negative allosteric modulator was [NS8593](#) (Fig 1), a chiral 2-
89 aminobenzimidazole derivative able to inhibit K_{Ca}2 channels at nanomolar

90 concentrations with no subtype selectivity (Strøbæk et al., 2006; Sørensen et al., 2008).
91 The negative modulation of NS8593 relies in the compound's ability to increase Ca^{2+}
92 EC_{50} for $\text{K}_{\text{Ca}2}$ activation and its binding site has been found to be in the inner pore
93 vestibule of the channel (Jenkins et al., 2011).

94 $\text{K}_{\text{Ca}2}$ channels are widely expressed in the CNS (Stocker and Pedarzani, 2000) and
95 therefore one of the challenges encountered during the development of compounds
96 targeting peripheral $\text{K}_{\text{Ca}2}$ is potential CNS mediated adverse effects (Habermann, 1984).
97 It is thus important to develop compounds with reduced blood brain barrier penetrance
98 in order to avoid possible adverse effects. In this work, we present a novel $\text{K}_{\text{Ca}2}$
99 negative allosteric modulator, AP14145 (Fig 1), a structurally close analogue of
100 NS8593 designed to inhibit specifically peripheral $\text{K}_{\text{Ca}2}$ channels by preventing its entry
101 in the CNS. In contrast to NS8593, it does not appear to have any immediate CNS
102 effects when dosed to rodents and therefore represents a new and improved tool
103 compound for studying $\text{K}_{\text{Ca}2}$ channel inhibition in rodents *in vivo*.

104

105 **Methods**

106 *Molecular biology*

107 r $\text{K}_{\text{Ca}2.3}$ WT (wild type) and r $\text{K}_{\text{Ca}2.3}$ S508T A533V were inserted in pXOON plasmids.
108 The r $\text{K}_{\text{Ca}2.3}$ NS8593 insensitive mutant was obtained by introducing the double point
109 mutation to the WT r $\text{K}_{\text{Ca}2.3}$ with the oligonucleotides
110 CCATAGCCAATggtAAGGAACGTGATG for S508T and
111 CATCATGGGTgtaGGCTGCACTGCCCTC for A533V, using PfuUltra II Fusion
112 polymerase (Agilent, USA) and T4 ligase (New England Biolabs, USA). Note that S508
113 and A533 on the r $\text{K}_{\text{Ca}2.3}$ are the equivalent positions of S507 and A532 on the h $\text{K}_{\text{Ca}2.3}$
114 channel. Competent *E. coli* were transformed using an aliquot of the mutagenesis
115 product by thermic shock and the plasmid DNA was purified using standard methods.
116 The h $\text{K}_{\text{Ca}3.1}$ T250S V275A mutant was kindly donated by Dorte Strøbæk. All
117 constructs were verified by sequencing.

118 *Cell culture and cell preparation*

119 To study the effect of AP14145 on the h $\text{K}_{\text{Ca}1.1}$ and h $\text{K}_{\text{Ca}2.x}$ channels we used four
120 different stable HEK293 cell lines expressing h $\text{K}_{\text{Ca}1.1}$, h $\text{K}_{\text{Ca}2.1}$, h $\text{K}_{\text{Ca}2.2}$ or h $\text{K}_{\text{Ca}2.3}$

121 channels obtained from NeuroSearch A/S (Ballerup, Denmark). The cell lines were
122 established as described in Strøbæk et al., 2004. For the identification of the binding
123 determinants of AP14145, wild-type HEK293 cells were transiently co-transfected with
124 rK_{Ca}2.3 WT, rK_{Ca}2.3 S508T A533V, hK_{Ca}3.1 WT or hK_{Ca}3.1 T250S V275A and 0.1 µg
125 of eGFP plasmid DNA using standard Lipofectamine™ (Thermo Fisher, USA)
126 protocols. Between one or two days after the transfection, patch clamp experiments
127 were conducted. The cells were cultured in Dulbecco's modified Eagle's medium
128 (DMEM1965, Thermo Fisher, USA) supplemented with 26.2 mM L⁻¹ NaHCO₃, 25 mM
129 L⁻¹ HEPES, 10 ml L⁻¹ Glutamax (Gibco, USA), 10 % foetal bovine serum (Biowest,
130 France) and 100 U ml⁻¹ of penicillin/streptomycin (Sigma, Germany). In the case of the
131 stable cell lines, 100 µg ml⁻¹ geneticin (Gibco, USA) were added to the medium. On the
132 day of the experiment, cells were detached from the flask using 1 ml of Detachin™
133 (Amsbio, United Kingdom). After being washed with free calcium and magnesium PBS
134 the cells were plated on 0.5 mm Ø coverslips. In the case of inside-out patch clamp, the
135 coverslips were treated overnight at 37°C with 50 mg ml⁻¹ poly-L-lysine (Sigma,
136 Germany) to get firmer cell attachment.

137 *Solutions and drugs*

138 K_{Ca}2 and K_{Ca}3.1 patch-clamp experiments were conducted using symmetrical K⁺
139 solutions. The extracellular solution contained 0.1 mM L⁻¹ CaCl₂, 3 mM L⁻¹ MgCl₂, 154
140 mM L⁻¹ KCl, 10 mM L⁻¹ HEPES and 10 mM L⁻¹ glucose (pH = 7.4 and 285 - 295
141 mOsm). The intracellular solution contained 8.106 mM L⁻¹ CaCl₂ (final free Ca²⁺
142 concentration of 400 nM L⁻¹), 1.167 mM L⁻¹ MgCl₂, 10 mM L⁻¹ EGTA, 154 mM L⁻¹
143 KCl, 10 mM L⁻¹ HEPES, 31.25/10 mM L⁻¹ KOH/EGTA and 15 mM L⁻¹ KOH (pH =
144 7.2). In addition, to study the activation of the channel with or without the presence of
145 AP14145 we used a range of intracellular solutions containing different free Ca²⁺
146 concentrations (0.01 - 30 µM L⁻¹). The composition of these intracellular solutions was
147 determined as described in Strobaek *et al.*, 2006.

148 For K_{Ca}1.1 the extracellular solution contained 2 mM L⁻¹ CaCl₂, 1 mM L⁻¹ MgCl₂, 145
149 mM L⁻¹ NaCl, 4 mM L⁻¹ KCl, 10 mM L⁻¹ HEPES and 10 mM L⁻¹ glucose (pH = 7.4 and
150 285 - 295 mOsm). The intracellular solution contained 5.374 mM L⁻¹ CaCl₂ (final free
151 Ca²⁺ concentration of 100 nM L⁻¹), 1.75 mM L⁻¹ MgCl₂, 120 mM L⁻¹ KCl, 10 mM L⁻¹
152 HEPES, 31.25/10 mM L⁻¹ KOH/EGTA (pH = 7.2).

153 The osmolarity of the intracellular solutions was adjusted using sucrose (Sigma,
154 Germany) to match the extracellular solutions.

155 AP14145 (*N*-(2-[[$(1R)^{-1}$]-[3-(trifluoromethyl)phenyl]ethyl]amino)⁻¹*H*¹,3-benzodiazol-4-
156 yl)acetamide) was synthesized by Syngene (India) as described in WO 2013104577 A1.
157 For *in vitro* experiments, AP14145 was solubilized in pure DMSO (Sigma-Aldrich,
158 Germany) at 10 mM L⁻¹ stock solutions. These stock solutions were stored at -20°C and
159 aliquots were solubilized at the desired concentration on the day of the experiment. For
160 *in vivo* experiments, 5 mg ml⁻¹ AP14145 were dissolved in a vehicle consisting of 50%
161 polyethylene glycol (PEG) 400 (Merck, Germany) and 50% sterile saline (PanReac
162 AppliChem, Germany) for infusion and the solution was sterile filtered (Nalgene, Rapid
163 flow 90 mM L⁻¹ filter unit, Thermo Scientific, USA) before use. The K_{Ca}1.1 selective
164 inhibitor [paxilline](#) was purchased from Sigma-Aldrich (Germany).

165 *Electrophysiology*

166 Patch clamp recordings were made using a HEKA EPC9 amplifier and the Patchmaster
167 software (HEKA Elektronik, Germany) at room temperature. Patch pipettes were pulled
168 using a horizontal DMZ Universal Puller (Zeitz, Germany) with resistances of 2.5 ± 0.1
169 M Ω for whole-cell patch clamp and 2.2 ± 0.6 M Ω for inside-out patch clamp. K_{Ca}2 and
170 K_{Ca}3.1 currents were elicited every 2 seconds using a 200 ms voltage ramps ranging -80
171 mV to +80 mV from a holding potential of 0 mV. K_{Ca}1.1 currents were elicited every 2
172 seconds using a 200 ms voltage ramps ranging -80 mV to +50 mV from a holding
173 potential of 0 mV. Data were sampled at 10 kHz. Series resistance values were 5.4 ± 0.6
174 M Ω with 80% of compensation. Two Bessel filters of 10 kHz and 2.9 kHz were used to
175 avoid background noise.

176 *Plasma Protein Binding*

177 Plasma protein binding (PPB) was experimentally determined by Syngene International
178 (India) in rat plasma using rapid equilibrium dialysis.

179 *Ex vivo experiments*

180 *Ex vivo* and *in vivo* experiments were performed under a license from the Danish
181 Ministry of justice (license No 2013⁻¹5-2934/00964) and in accordance with the Danish
182 guidelines for animal experiments according to the European Commission Directive
183 86/609/EEC. The animals were housed in groups of 2-4 in high-top cages with bedding

184 (wood shavings) and under constant climatic conditions (22°C) at the Department of
185 Experimental Medicine, University of Copenhagen. The animals were kept at a 12 hour
186 light-dark cycle with ad libitum access to clean water and standard laboratory rodent
187 diet.

188 *Isolated perfused heart preparation*

189 Rats express K_{Ca2} channels in the atria, and have previously been used to study the
190 effect of K_{Ca2} inhibition on atrial refractoriness. Male Sprague-Dawley rats (250 - 350
191 g, 1-3 months old, Janvier Labs, France) were anaesthetized with fentanyl-midazolam
192 mixture, 5 mg ml⁻¹ dose 0.3 mL/100 g BW, s.c. A tracheotomy was performed in the
193 ventilated rat. The aorta was cannulated and the heart was excised, and connected to a
194 Langendorff retrograde perfusion setup (Hugo Sachs Elektronik, Harvard Apparatus
195 GmbH, Germany). The heart was retrogradely perfused with Krebs–Henseleit buffer (in
196 mM L⁻¹: NaCl 120.0, NaHCO₃ 25.0, KCl 4.0, MgSO₄ 0.6, NaH₂PO₄ 0.6, CaCl₂ 2.5,
197 Glucose 11.0, saturated with 95% O₂ and 5% CO₂, 37°C, pH 7.4) at a constant
198 perfusion pressure of 80 mmHg. The electrical activity of the heart was measured by
199 volume conducted electrocardiograms (ECGs) and the atrial epicardial monophasic
200 action potentials by an electrode on the right atrium. The signal was sampled at 1 kHz
201 (PowerLab systems, ADInstruments, UK) and monitored by using LabChart 7 software
202 (ADInstruments, UK). The hearts were immersed into a temperature-controlled and
203 carbonated bath containing Krebs–Henseleit buffer. A bipolar pacing electrode was
204 placed on the right atria in order to stimulate the heart and measure the AERP, which
205 was defined as the longest S1-S2 interval failing to elicit an action potential. The AERP
206 was measured every five minutes by applying electrical stimulation (2 times rheobase)
207 with a fixed interval of 133 ms (S1 stimulation) and for every 10th beat an extra stimulus
208 (S2 stimulation) was applied with 1 ms increments.

209 Baseline recordings were made for at least 20 minutes and continued until the ECG
210 morphology and AERP recording were stable. After the baseline recording, four 20-
211 minute episodes followed in which, the heart, was perfused with: 1) 1 μM L⁻¹ paxilline
212 2) 3 μM L⁻¹ paxilline 3) washout 4) 10 μM L⁻¹ AP14145 and AERP measurements were
213 performed every fifth minute. Measurements after 20 minutes of drug perfusion or
214 washout were used for statistical analysis.

215 *In vivo experiments*

216 *Closed chest recording of atrial refractoriness in rats*

217 A total of 18 1-3 months old male Sprague-Dawley rats (Janvier, France) weighing 400-
218 550 g were anesthetized and randomly divided in three groups: one group receiving
219 AP14145 as bolus injections (n=6), a time matched control group receiving vehicle as
220 bolus injections (n=6), and a group receiving AP14145 as a constant-rate infusion
221 (n=6). The rats were anaesthetized with 3 % isofluran/oxygen and an intravenous
222 catheter was placed in the femoral vein for drug injection. Needle ECG electrodes were
223 placed in each limb for ECG recordings (ADInstruments, UK). The temperature of the
224 rats was monitored and kept stable during the experiment with a heating lamp (37 °C).
225 A catheter with eight electrodes (Millar Inc., US) was placed in the right atrium of an
226 anaesthetized rat via the jugular vein. Two of the electrodes were used to pace the
227 atrium and six electrodes were used to measure the electrical activity in the atrium. This
228 combination allows measurements of the AERP and the changes in AERP as a
229 consequence of injection of the test compound. Once the experiment was completed,
230 rats were euthanized by a mixture of 200 mg ml⁻¹ pentobarbital and 20 mg ml⁻¹
231 lidocaine hydrochloride (Glostrup Apotek, Denmark) i.v. injection. Since the risk of
232 placebo effect and subjective interpretation of the results was inexistent or minimal, no
233 blinding was used.

234 *Measurement of AERP*

235 Each experiment lasted for at least 60 minutes and was divided into three 20-minutes
236 episodes. During the entire experiment the ECG was monitored. The AERP was
237 measured by applying electrical stimulation (5 times rheobase) with a fixed interval of
238 120 ms (S1 stimulation) and for every 10th beat an extra stimulus (S2 stimulation) was
239 applied with 1 ms increments. The AERP was defined as the longest S1-S2 interval
240 failing to elicit an action potential. Between the AERP recordings, the heart remained
241 unpaced. Baseline AERP recordings with no compound present were made every 5th
242 minute for 20 minutes before adding test compound.

243 *Increasing bolus dosing*

244 After the baseline recording, two 20-minute episodes followed in which two groups of
245 rats (n=6 each) were injected with increasing doses of AP14145 (2.5 mg kg⁻¹ and 5.0
246 mg kg⁻¹) or equivalent volumes of vehicle (50% PEG-400 and 50% saline). The

247 injection time was 30 seconds. AERP was measured 1, 5, 10 and 15 minutes after the
248 start of each injection.

249 *Constant rate infusion of AP14145*

250 After the baseline recording, a third group of rats received a constant rate infusion of 40
251 mg kg⁻¹ h⁻¹ AP14145 over 20 minutes followed by a 20-minute post-infusion period. In
252 these animals the AERP was measured every 2 minutes during and after infusion.

253 *Beam walk test - assessment of motor balance and coordination in mice*

254 A beam walk test was performed in mice in order to assess CNS exposure of K_{Ca}2
255 inhibitors in vivo. The mouse beam walk test is a validated test for addressing motor
256 function (Brooks and Dunnett, 2009). Three groups of 1-2 months old male NMRI mice
257 (Taconic Biosciences, USA) weighing 23-49 g were used. The mice were randomly
258 assigned to either the vehicle control group, a 10 mg kg⁻¹ NS8593 or a 10 mg kg⁻¹
259 AP14145 group. The mice were placed on a 1 meter wooden beam (ø 12 mm) and
260 briefly trained in crossing the beam. After training, a 1 minute baseline recording was
261 initiated and the number of falls and slips were noted. Hereafter the mice were
262 randomly assigned to receive K_{Ca}2 inhibitors or vehicle (50% PEG-400 and 50% saline)
263 by i.v. bolus injection in the tail vein. The mouse was observed immediately after
264 injection for any behavioural changes. If any adverse effects occurred, the mouse was
265 euthanized. Otherwise the mice were observed for behavioural changes and challenged
266 with the beam walk 12 minutes post injection. All experiments were documented by
267 video recordings.

268 *Data analysis*

269 Data was extracted from PatchMaster and analysed using GraphPad Prism 7.

270 To calculate the IC₅₀ value of AP14145, the measured currents were first normalized.
271 Recorded currents without the presence of the drug were used as baseline and currents
272 recorded at the highest tested concentration of AP14145 (30 µM L⁻¹) were used as total
273 inhibition of the channel. Individual IC₅₀ values for each experiment were calculated
274 using the equation:

$$Y = Y_{min} + \frac{(Y_{max} - Y_{min})}{1 + 10^{X - \log IC_{50}}}$$

275 where X is the log of dose of AP14145 and Y is the normalized measured current. In all
276 cases a Hill slope of -1.0 was considered. Individual IC₅₀ values were later used to
277 obtain the final $\bar{x} \pm \text{SEM}$. IC₅₀. The individual IC₅₀ values were then used in student's t-
278 tests to determine subtype selectivity.

279 To calculate the EC₅₀ of calcium, the values were normalized using the currents
280 recorded at the lowest calcium concentration (0.01 $\mu\text{M L}^{-1}$) for total inactivation and at
281 the highest calcium concentration (30 $\mu\text{M L}^{-1}$) for maximum activation of the channel.
282 Individual EC₅₀ values for each experiment were calculated using the equation:

$$Y = Y_{min} + \frac{(Y_{max} - Y_{min})}{1 + 10^{(\log EC_{50} - X) \times HillSlope}}$$

283 where X is the log of dose of calcium and Y is the normalized measured current with
284 variable Hill slope. Individual EC₅₀ values were used to determine the final $\bar{x} \pm \text{SEM}$
285 EC₅₀.

286 Currents were also normalized to assess and compare the inhibitory effect of 10 $\mu\text{M L}^{-1}$
287 AP14145 on HEK cells expressing K_{Ca}1.1, K_{Ca}2.1, K_{Ca}2.2, K_{Ca}2.3, K_{Ca}2.3 S508T
288 A532V, K_{Ca}3.1 or K_{Ca}3.1 T250S V275A. For each individual cell, 0% current was
289 defined as 0 nA and 100% current was defined as the current recorded in the absence of
290 the compound. The final results are summarized as $\bar{x} \pm \text{SEM}$ of the individual values.

291 To quantify and compare the activation and inhibition effects of 10 $\mu\text{M L}^{-1}$ NS309 and
292 10 $\mu\text{M L}^{-1}$ AP14145 on the K_{Ca}2.3 channel, values were normalized for each individual
293 cell. In this case, 0 was defined as 0 nA and currents recorded in the absence of both
294 compounds were defined as 1. These individual values were used to calculate the final \bar{x}
295 $\pm \text{SEM}$.

296 The last ten data points obtained after the application of a new compound or solution
297 and corresponding to the steady state were used to create every single value.

298 Student's t-test was performed to assess statistical significance of the effect of
299 AP14145. P values < 0.05 were considered significant.

300 Physicochemical properties of AP14145 and NS8593 were calculated using the Instant
301 JChem (ChemAxon) software.

302 Perfused rat heart data and closed chest continuous data are summarized using the $\bar{x} \pm$
303 SEM. A one-way ANOVA with Tukey's comparison post-test was used to compare the

304 effect of paxilline and AP14145 on the isolated rat heart. Multiple t tests with Holm-
305 Sidak's correction for multiple comparisons were used to compare AERP differences
306 between the group of rats that received AP14145 as increasing bolus doses and the time
307 matched control group at matching time points. Multiple t tests with Holm-Sidak's
308 correction for multiple comparisons were used to compare each AERP-value during and
309 after infusion to the mean baseline AERP values. P values < 0.05 were considered
310 significant.

311 *Nomenclature of Targets and Ligands*

312 Key protein targets and ligands in this article are hyperlinked to corresponding entries in
313 <http://www.guidetopharmacology.org>, the common portal for data from the
314 IUPHAR/BPS Guide to PHARMACOLOGY (Southan et al., 2016), and are
315 permanently archived in the Concise Guide to PHARMACOLOGY 2015/16 (Alexander
316 et al., 2015).

317

318 **Results**

319 *AP14145 inhibits both hK_{Ca}2.2 and hK_{Ca}2.3 currents with equal potency*

320 Using inside-out manual patch clamp we tested AP14145 on both the hK_{Ca}2.2 and
321 hK_{Ca}2.3 channels. Once the patch was excised, the channels were exposed to the bath's
322 intracellular solution, containing 400 nM L⁻¹ free [Ca²⁺]. In symmetrical intra- and
323 extra-cellular K⁺ solutions, hK_{Ca}2.3 currents displayed a characteristic inwardly
324 rectifying current-voltage relationship (Fig 2a). Currents were elicited using voltage
325 ramps from -80 mV to +80 mV applied every 2 seconds. Once the hK_{Ca}2 current was
326 stable, up to 8 increasing concentrations of AP14145 between 0.01 - 30 μM L⁻¹ were
327 applied and perfused by gravity flow on the patch (Fig 2b). For each concentration the
328 drug was applied until steady state was reached.

329 AP14145 was able to inhibit both hK_{Ca}2.2 and hK_{Ca}2.3 in a concentration-dependent
330 fashion (Fig 2b, data not shown for hK_{Ca}2.2). The effect started at nanomolar
331 concentrations and total inhibition was reached at 30 μM L⁻¹ (Fig 2b). Calculated IC₅₀
332 for AP14145 on both the hK_{Ca}2.2 and hK_{Ca}2.3 was 1.1 ± 0.3 μM L⁻¹ (n = 7 each, Fig
333 2c), with a fixed Hill slope of -1.0. The drug consequently did not display any subtype
334 selectivity between hK_{Ca}2.2 and hK_{Ca}2.3.

335 Additionally, the inhibitory effect of AP14145 was also tested on the hK_{Ca}1.1, hK_{Ca}2.1
336 and hK_{Ca}3.1 channels using whole cell patch clamp for further selectivity assessment
337 (Fig 3). The application of 10 μM L⁻¹ AP14145 inhibited 50 ± 10% of the hK_{Ca}1.1
338 current (n = 6) and 90 ± 4% of the hK_{Ca}2.1 current (n = 7). In contrast, hK_{Ca}3.1 currents
339 were not significantly affected by the application of 10 μM L⁻¹ AP14145 (n = 8).

340 *AP14145 modifies hK_{Ca}2.3 calcium sensitivity*

341 To establish how AP14145 inhibits the channel, we performed inside out patch clamp
342 recordings to assess the effect of the drug on the calcium sensitivity of the hK_{Ca}2.3
343 channel. Patches were excised from HEK cells stably expressing the hK_{Ca}2.3 channel
344 and currents elicited using voltage ramps. We exposed the patches to eight different free
345 Ca²⁺ concentrations and calculated the EC₅₀ for calcium activation of the channel in the
346 absence and presence of 10 μM L⁻¹ AP14145 (Fig 4a and b). Free calcium
347 concentrations ranged from 0.01 - 30 μM L⁻¹ and were perfused using gravity flow.
348 Solutions were applied until steady state was reached.

349 In the absence of AP14145, hK_{Ca}2.3 channels were fully activated at 3 μM L⁻¹ of
350 intracellular Ca²⁺ (Fig 4a), but in the presence of 10 μM L⁻¹ AP14145, up to 10 μM L⁻¹
351 were needed to reach total activation of the channel (Fig 4b). At a 10 μM L⁻¹
352 concentration, the drug shifted the calcium-activation curve of the K_{Ca}2.3 channel to the
353 right (Fig 4c), so higher calcium concentrations were needed to activate the channels.
354 This was also shown by the significantly increased EC₅₀ of Ca²⁺ from 0.36 ± 0.02 μM L⁻¹
355 (n = 9) to 1.3 ± 0.2 μM L⁻¹ (n = 7). Most prominently, the Hill coefficients were also
356 significantly modified by the presence of AP14145 from 5.2 ± 0.3 to 1.2 ± 0.1 (absence
357 of AP14145 vs. 10 μM L⁻¹ AP14145).

358 *AP14145 reverses the effect of the positive K_{Ca}2 gating modulator [NS309](#)*

359 The inhibitory effect of AP14145 was also studied in the presence of a high
360 concentration of the K_{Ca}2 positive gating modulator NS309. Patches excised from HEK
361 cells stably expressing the hK_{Ca}2.3 channel were exposed to 400 nM L⁻¹ free [Ca²⁺]
362 intracellular solution. After stabilisation of the baseline, 10 μM L⁻¹ NS309 were applied
363 on the patch, further activating the channel and increasing hK_{Ca}2.3 current by 4 ± 1 fold
364 (n = 7, Fig 5). When steady state was reached, 10 μM L⁻¹ AP14145 were added to the
365 bath, in the continued presence of NS309. The application of AP14145 reduced hK_{Ca}2.3
366 current to values close to the control baseline, reversing the positive gating effect of

367 NS309 (Figure 5). Furthermore, in the presence of $10 \mu\text{M L}^{-1}$ NS309, total current
368 inhibition by $10 \mu\text{M L}^{-1}$ AP14145 was significantly diminished from $80 \pm 3\%$ ($n = 7$) to
369 $61 \pm 4\%$ ($n = 7$, Fig 5).

370 *AP14145 inhibition strongly depends on two amino acids, S508 and A533, located in*
371 *the inner pore of the channel*

372 To establish possible molecular determinants of $\text{rK}_{\text{Ca}2.3}$ inhibition by AP14145 we
373 mutated two amino acids, S508 and A533 (corresponding to S507 and A532 in
374 $\text{hK}_{\text{Ca}2.3}$), located in the inner pore of the channel and known to confer sensitivity to the
375 negative allosteric modulator of $\text{K}_{\text{Ca}2}$ channels, NS8593 (Jenkins et al., 2011).

376 Whole-cell patch clamp experiments were conducted on transiently transfected HEK
377 cells with either the WT $\text{rK}_{\text{Ca}2.3}$ channel or the $\text{rK}_{\text{Ca}2.3}$ S508T A533V mutant. The
378 channels were activated by 400 nM L^{-1} free $[\text{Ca}^{2+}]$ intracellular solution and currents
379 were elicited using voltage ramps. Again, in symmetrical intra- and extra-cellular K^+
380 solutions, WT $\text{rK}_{\text{Ca}2.3}$ currents displayed a characteristic inwardly rectifying current-
381 voltage relationship (Fig 6a). In contrast to the WT $\text{rK}_{\text{Ca}2.3}$ channel, the maximum
382 current normalized to cell capacitance of the mutant $\text{rK}_{\text{Ca}2.3}$ was significantly reduced
383 (WT: $650 \pm 96 \text{ pA/pF}$ vs. mutant: $87 \pm 23 \text{ pA/pF}$, $n = 7$ each, Fig 6b). Rectification,
384 determined as the ratio of the current amplitude at -80 and $+80 \text{ mV}$, was also changed
385 by the mutation, from $9 \pm 1 I_{-80}/I_{+80}$ in the WT to $2.9 \pm 0.4 I_{-80}/I_{+80}$ in the mutant. These
386 observations are in agreement with what was previously described by Jenkins *et al.*,
387 2011. After current stabilisation, $10 \mu\text{M L}^{-1}$ of AP14145 were applied on the cell
388 transfected with the WT or the mutant protein for 1 - 2 min or until a steady state drug
389 effect was reached (Fig 6a and b).

390 The experiments showed that, while $\text{rK}_{\text{Ca}2.3}$ currents recorded from cells transfected
391 with the WT channel were strongly inhibited by application of $10 \mu\text{M L}^{-1}$ AP14145 (Fig
392 6a), currents recorded from cells transfected with the mutant $\text{rK}_{\text{Ca}2.3}$ were only
393 partially affected by the presence of the compound (Fig 6b). The inhibitory effect of
394 AP14145 was statistically different between the WT and the mutant when analysed as
395 the relative current inhibition after application of AP14145 ($95 \pm 1\%$ and $22 \pm 6\%$
396 inhibition, WT $\text{rK}_{\text{Ca}2.3}$ vs $\text{rK}_{\text{Ca}2.3}$ S508T A533V, $n = 7$ each, Fig 6e).

397 To ensure that S508 and A533 are important for AP14145 sensitivity, we introduced
398 these amino acids in their homologous positions in the AP14145 insensitive $\text{K}_{\text{Ca}3.1}$

399 channel, T250 and V275, respectively. The $K_{Ca3.1}$ T250S V275A mutant was tested
400 using whole cell patch clamp to determine its sensitivity to AP14145. After activation
401 of the channel with 400 nM L^{-1} free $[Ca^{2+}]$ intracellular solution and current
402 stabilization, $10 \text{ } \mu\text{M L}^{-1}$ AP14145 was applied on the cell. In contrast to the $K_{Ca3.1}$ WT
403 channel (Fig 6c), the mutant $K_{Ca3.1}$ current was inhibited by $92 \pm 1 \%$ ($n=7$, Fig 6d),
404 comparable to the inhibitory effect observed on $rK_{Ca2.3}$.

405 *AP14145 increases the duration of the atrial effective refractory period in isolated*
406 *perfused rat hearts*

407 Excised rat hearts were connected to a retrograde perfusion Langendorff setup to
408 measure the effect of AP14145 on the AERP and discard any $K_{Ca1.1}$ mediated effects.

409 Once a stable baseline was achieved, the hearts were perfused first with $1 \text{ } \mu\text{M L}^{-1}$ of the
410 $K_{Ca1.1}$ inhibitor paxilline. Twenty minutes later, the dose of paxilline was increased to 3
411 $\text{ } \mu\text{M L}^{-1}$ for 20 more minutes. Finally, after a 20 minute wash period, $10 \text{ } \mu\text{M L}^{-1}$ of
412 AP14145 were perfused into the heart.

413 Paxilline did not affect the AERP in any of the tested doses, but AP14145 was able to
414 prolong the AERP significantly, from $19 \pm 3 \text{ ms}$ to $57 \pm 12 \text{ ms}$ ($n = 5$, Fig. 7).

415 *AP14145 increases the duration of the atrial effective refractory period in rats*

416 To investigate the *in vivo* effects of AP14145, 6 male rats received AP14145 in
417 increasing doses (2.5 mg kg^{-1} and 5 mg kg^{-1}) and 6 time matched control rats received
418 corresponding volumes of vehicle (0.5 ml kg^{-1} and 1 ml kg^{-1} , respectively).

419 One minute after injection of 2.5 mg kg^{-1} AP14145 the AERP was significantly
420 increased from $37 \pm 2 \text{ ms}$ in the time matched control group to $53 \pm 6 \text{ ms}$ (Fig. 8a). The
421 AERP returned towards baseline values, and five minutes after the injection of 2.5 mg
422 kg^{-1} the AERP was no longer significantly different from that of the time matched
423 controls. One minute after injection of 5 mg kg^{-1} AP14145 the AERP was significantly
424 increased from $31 \pm 2 \text{ ms}$ in the time matched control group to $58 \pm 8 \text{ ms}$ (Fig. 8a).
425 Again, the AERP returned towards baseline values, and ten minutes after the injection
426 of 5 mg kg^{-1} the AERP was no longer significantly different from that of the time
427 matched controls.

428 A third group of rats ($n = 6$) received a constant rate infusion of $40 \text{ mg kg}^{-1} \text{ h}^{-1}$ over 20
429 minutes and were monitored for an additional 20 minutes after infusion (Fig 8b). In

430 these rats the AERP was significantly increased compared to baseline values from 4
431 minutes after the infusion started (i.e. after a cumulative dose of 2.7 mg kg⁻¹). The
432 AERP continued to increase during the rest of the infusion and returned towards
433 baseline values after infusion.

434 *AP14145 does not impair motor coordination in mice*

435 A beam walk test was performed in mice in order to assess CNS exposure of K_{Ca}2
436 inhibitors *in vivo*. Three groups of male NMRI mice were used, a vehicle control group
437 (30.5 ± 0.3 g, n = 6), a 10 mg kg⁻¹ NS8593 (26 ± 1 g, n = 3) and a 10 mg kg⁻¹ AP14145
438 group (36 ± 5 g, n = 6).

439 Shortly after the injection of 10 mg kg⁻¹ NS8593, all mice showed severe convulsions
440 making them unable to walk on the beam (Fig 9). Therefore, the mice were euthanized
441 by cervical dislocation and the experiment was terminated.

442 In contrast, when mice were injected with AP14145, no acute effects were observed and
443 the beam walk test was performed 12 minutes after dosing. The mice did not slip or fall
444 from the beam in either of the two tests and no behavioural changes were observed.
445 These observations were not different to the ones from the vehicle control group (Fig 9).

446

447 **Discussion**

448 K_{Ca}2 channels are inwardly rectifying potassium channels (Köhler et al., 1996) widely
449 distributed in humans, both in the CNS and peripheral tissues (Chen et al., 2004). In the
450 heart, they play an important role in the late repolarization phase of the atria (Li et al.,
451 2009). Moreover, it has been demonstrated that inhibition of K_{Ca}2 channels prolongs the
452 AERP (Diness et al., 2010; Skibsbye et al., 2011; Qi et al., 2014; Haugaard et al.,
453 2015). Therefore, the K_{Ca}2 channel is considered a promising new target to treat AF.
454 Here we present a new K_{Ca}2 inhibitor, AP14145, which could constitute an important
455 tool in rodents, to target and study the inhibition of peripheral K_{Ca}2.x channels *in vivo*.

456 In initial experiments it was established that AP14145 inhibits hK_{Ca}2.2 and hK_{Ca}2.3 in
457 an equipotent manner with IC₅₀ values of 1.1 ± 0.3 μM L⁻¹. To determine the
458 mechanism of inhibition of AP14145, we conducted inside-out patch clamp
459 experiments. Patches were excised from HEK 293 cells stably expressing the hK_{Ca}2.3
460 channel and exposed to a range of intracellular solutions with different free calcium

461 concentrations. Calcium activation was assessed in the absence and presence of
462 AP14145. The compound significantly increased the EC_{50} of Ca^{2+} from $0.36 \pm 0.02 \mu M$
463 L^{-1} to $1.3 \pm 0.2 \mu M L^{-1}$, thereby shifting the Ca^{2+} activation curve of K_{Ca2} channel
464 activation to higher values. The Hill coefficients were also modified by the presence of
465 AP14145 from 5.2 ± 0.3 to 1.2 ± 0.1 (absence of AP14145 vs. $10 \mu M L^{-1}$ AP14145).
466 These results suggest that the drug modifies the channel's calcium sensitivity and acts
467 as a negative allosteric modulator, very similar to the previously reported NS8593. The
468 change of the Hill coefficient may also indicate a loss of calcium cooperativity which
469 may impede calcium binding. Moreover, the inhibitory effect of AP14145 was studied
470 in the presence of the $K_{Ca2.x}$ positive allosteric modulator NS309, which is known to
471 increase the calcium sensitivity of the channel (Strøbæk et al., 2004). In these
472 experiments, AP14145 was able to reverse NS309-mediated $K_{Ca2.3}$ channel activation,
473 suggesting a functional competition between the two compounds and further supporting
474 the negative allosteric mechanism of AP14145.

475 In the study by Jenkins *et al.* in 2011, the binding site of NS8593, another K_{Ca2} negative
476 allosteric modulator, was found to be located at the inner pore of the channel. This was
477 an interesting finding since the drug had previously been found to decrease calcium
478 sensitivity of the channel and could be speculated to locate the binding site at the C-
479 terminal domain, close to the calmodulin binding domain. Instead, binding interacts
480 with two specific amino acids S507 and A532, located on helices S5 and S6,
481 respectively. When these two amino acids were mutated to the corresponding residues
482 found on the closely related $K_{Ca3.1}$ channel, which is not inhibited by NS8593, they
483 obtained a $K_{Ca2.3}$ mutant resistant to the effect of the drug, with preserved channel
484 confirmation and calcium sensitivity. In order to find out if AP14145 and NS8593
485 shared the same binding site, we conducted whole cell patch clamp experiments on
486 transiently transfected HEK cells with r $K_{Ca2.3}$ WT or r $K_{Ca2.3}$ S508T A533V,
487 corresponding to S507 and A532 in the h $K_{Ca2.3}$ channel. While the WT current was
488 strongly inhibited using $10 \mu M L^{-1}$ AP14145, the NS8593 resistant mutant was only
489 partially affected by the presence of the drug, suggesting that S508 and A533 are
490 important also for AP14145 inhibition. The loss of AP14145 sensitivity in r $K_{Ca2.3}$
491 S508T A533V cannot be explained by differences in calcium-activation or channel
492 conformation as these characteristics are preserved in the mutant (Jenkins et al., 2011).
493 AP14145 and NS8593 are structurally close analogues (Fig 1) and these experiments

494 demonstrate that AP14145 and NS8593 appear to share the same inhibition mechanism
495 as well as some of their binding determinants. Finally, to confirm that S507 and A532
496 are important for the inhibitory effect of AP14145 on $K_{Ca2.3}$ we introduced these amino
497 acids in their homologous positions on the insensitive $K_{Ca3.1}$ channel. With the addition
498 of these two amino acids, AP14145 sensitivity was fully restored in the $K_{Ca3.1}$ channel
499 (Fig 6), further demonstrating that S507 and A532 are important for AP14145
500 inhibition. K_{Ca2} channels are widely expressed in the brain, including the cerebellum
501 (Stocker and Pedarzani, 2000), where they contribute to the action potential
502 afterhyperpolarization (Hosy et al., 2011). It has further been demonstrated that
503 inhibition of $K_{Ca2.2}$ channels in cerebellum disturbs the motor output which is revealed
504 as ataxia or convulsion like phenotype especially apparent in the hind legs (Alvina and
505 Khodakhah, 2010). As an indication of CNS exposure and inhibition of central K_{Ca2}
506 channels a beam walk test was performed. The test is designed to assess impaired motor
507 coordination and balance in mice.

508 Mice injected intravenously with 10 mg kg^{-1} NS8593 immediately showed acute CNS
509 effects in the form of convulsions, and consequently were euthanized. In contrast i.v.
510 injection of 10 mg kg^{-1} AP14145 had no apparent CNS effects, and the mice were able
511 to cross the beam without slipping or falling from the beam, similarly to the vehicle
512 control mice. Importantly, NS8593 plasma protein binding is higher than AP14145
513 (95.38% vs. 91.35% bound, respectively, Table 1), meaning that a higher amount of
514 AP14145 is freely available in plasma compared to NS8593 when the same dose of both
515 compounds is injected. Moreover, we found that i.v. injection of 2.5 mg kg^{-1} AP14145
516 significantly increases the atrial refractoriness in rats within 1 min of injection,
517 suggesting that 10 mg kg^{-1} is sufficient to peripheral K_{Ca2} target engagement.

518 A possible explanation for the apparent difference in CNS penetration of the two
519 compounds lies in their structure (Fig 1) and physicochemical properties (Table 1). In
520 particular, AP14145 contains a carboxamide moiety on the bicyclic benzimidazole ring,
521 a chemical moiety that adds polarity to the molecule and is known to be a common
522 substrate for P-glycoprotein transporter mediated efflux. The calculated polar surface
523 area (PSA) of AP14145 is 70, which is significantly higher than NS8593 (Table 1),
524 indicating a lower likelihood of penetrating the blood-brain barrier. It can thus be
525 hypothesised that the structural features in AP14145 make the compound less likely to
526 penetrate to induce CNS mediated convulsions when compared to NS8593. Although

527 this difference in profile could in principle be caused by differences in the
528 pharmacokinetic profile of the two compounds, this seems an unlikely explanation,
529 since, as has been shown in Diness et al. (2010), 5 mg kg⁻¹ of NS8593 cause similar
530 increases of the AERP in rats when compared to the effect of 5 mg kg⁻¹ of AP14145
531 (Fig 8a).

532 High concentrations of AP14145 (10 μM L⁻¹) significantly inhibited the K_{Ca}1.1
533 channel. However, as paxilline, which is a well-known specific inhibitor of K_{Ca}1.1
534 channels (Nardi and Olesen, 2008), did not have any effect on the atrial refractoriness of
535 isolated perfused rat hearts, we conclude that the inhibition of K_{Ca}1.1 by AP14145 does
536 not contribute to the AERP prolonging effects of AP14145. This is in accordance with
537 studies demonstrating the lack of K_{Ca}1.1 channels and currents in the plasma membrane
538 of cardiomyocytes (Bautista et al., 2009; Singh et al., 2013).

539 The apparent reduced CNS exposure of the drug makes AP14145 a unique and useful
540 new tool compound that allows the study of peripheral K_{Ca}2 inhibition without
541 apparently interfering with CNS function in awake rodents. This might help further
542 development and understanding of the cardiac and endothelial role of K_{Ca}2 in a number
543 of physiological and pathological settings.

544

545 **Conclusions**

546 In this work we present the novel K_{Ca}2 negative gating modulator AP14145. This new
547 drug inhibits both the hK_{Ca}2.2 and hK_{Ca}2.3 with equal potency (IC₅₀ = 1.1 ± 0.3 μM L⁻¹
548 with 400 nM L⁻¹ intracellular Ca²⁺) by decreasing the calcium sensitivity of the channel.
549 The inhibitory effect of AP14145 effect is strongly dependent on two amino acids, S508
550 and A533 in the rK_{Ca}2.3, located in the inner pore of the channel. *In vivo*, AP14145
551 significantly increases the atrial refractoriness in rats shortly after a 2.5 mg kg⁻¹ or 5.0
552 mg kg⁻¹ bolus injection. In contrast to NS8593, a dose of 10 mg kg⁻¹ of AP14145 did not
553 trigger any apparent acute CNS mediated effects in mice, suggesting that the compound
554 does not penetrate the blood brain barrier to the same degree as NS8593 in rodents. This
555 key difference could for the first time allow for the use of a K_{Ca}2 negative modulator *in*
556 *vivo* without interfering with CNS function. We expect this feature might help further
557 development and understanding of the cardiac and endothelial role of K_{Ca}2 channels.

558

559 **Author contributions**

560 *Rafel Simó-Vicens*: conception and design of the study, data acquisition
561 (electrophysiology and molecular biology) and analysis, drafting and critical revision of
562 the work.

563 *Jeppe E. Kirchhoff*: acquisition of data (closed chest recordings), data analysis, drafting
564 and critical revision of the work.

565 *Lea Abildgaard Jensen*: acquisition of data (beam walk test and perfused heart
566 preparation), data analysis, drafting and critical revision of the work.

567 *Bernardo Dolce*: data acquisition (electrophysiology and molecular biology) and
568 analysis.

569 *Tobias Speerschneider*: acquisition of data (closed chest recordings), data analysis,
570 drafting and critical revision of the work.

571 *Ulrik S. Sørensen*: conception and design of AP14145, conception and design of the
572 study, drafting and critical revision of the work.

573 *Morten Grunnet*: conception and design of the study, critical revision of the work.

574 *Jonas G. Diness*: conception and design of the study, data analysis, drafting and critical
575 revision of the work.

576 *Bo H. Bentzen*: conception and design of the study, drafting and critical revision of the
577 work.

578

579 **Acknowledgements**

580 The study was supported by Innovation Fund Denmark, the Carlsberg Foundation, and
581 the European Union's Horizon 2020 research and innovation programme under the
582 Marie Skłodowska-Curie grant agreement No. 675351. We would also like to thank
583 Dorte Strøbæk for kindly donating the hK_{Ca}3.1 T250S V275A mutant.

584

585 **Conflicts of interest statement**

586 All authors of this study are or have been employed by Acesion Pharma.

587

588 **References**

589 Adelman, J.P. (2016). SK channels and calmodulin. *Channels 10*: 1–6.

590 Alexander, S., Catterall, W., Kelly, E., Marrion, N., Peters, J., Benson, H., et al. (2015).
591 The Concise Guide to PHARMACOLOGY 2015/16: Voltage-gated ion channels. *Br J*
592 *Pharmacol. 172*: 5904–5941.

593 Alvina, K., and Khodakhah, K. (2010). KCa channels as therapeutic targets in episodic
594 ataxia type-2. *J Neurosci 30*: 7249–7257.

595 Bautista, L., Castro, M.J., López-Barneo, J., and Castellano, A. (2009). Hypoxia
596 inducible factor-2 α stabilization and maxi-K⁺ channel β 1-subunit gene repression by
597 hypoxia in cardiac myocytes: Role in preconditioning. *Circ. Res. 104*: 1364–1372.

598 Brooks, S.P., and Dunnett, S.B. (2009). Tests to assess motor phenotype in mice: a
599 user's guide. *Nat. Rev. Neurosci. 10*: 519–29.

600 Chen, M.X., Gorman, S.A., Benson, B., Singh, K., Hieble, J.P., Michel, M.C., et al.
601 (2004). Small and intermediate conductance Ca²⁺-activated K⁺ channels confer
602 distinctive patterns of distribution in human tissues and differential cellular localisation
603 in the colon and corpus cavernosum. *Naunyn. Schmiedebergs. Arch. Pharmacol. 369*:
604 602–615.

605 Christophersen, I.E., Rienstra, M., Roselli, C., Yin, X., Geelhoed, B., Barnard, J., et al.
606 (2017). Large-scale analyses of common and rare variants identify 12 new loci
607 associated with atrial fibrillation. *Nat. Genet. 49*:

608 Diness, J.G., Bentzen, B.H., Sørensen, U.S., and Grunnet, M. (2015). Role of Calcium-
609 activated Potassium Channels in Atrial Fibrillation Pathophysiology and Therapy. *J.*
610 *Cardiovasc. Pharmacol. 66*: 441–8.

611 Diness, J.G., Sørensen, U.S., Nissen, J.D., Al-Shahib, B., Jespersen, T., Grunnet, M., et
612 al. (2010). Inhibition of small-conductance ca²⁺-activated k⁺ channels terminates and
613 protects against atrial fibrillation. *Circ. Arrhythmia Electrophysiol. 3*: 380–390.

614 Ellinor, P.T., Lunetta, K.L., Glazer, N.L., Pfeufer, A., Alonso, A., Chung, M.K., et al.

615 (2010). Common variants in KCNN3 are associated with lone atrial fibrillation. *Nat.*
616 *Genet.* 42: 240–244.

617 Habermann, E. (1984). Apamin. *Pharmac. Ther.* 25: 255–270.

618 Haugaard, M.M., Hesselkilde, E.Z., Pehrson, S., Carstensen, H., Flethøj, M.,
619 Præstegaard, K.F., et al. (2015). Pharmacologic inhibition of small-conductance
620 calcium-activated potassium (SK) channels by NS8593 reveals atrial antiarrhythmic
621 potential in horses. *Hear. Rhythm* 12: 825–835.

622 Hosy, E., Piochon, C., Teuling, E., Rinaldo, L., Hansel, C., and Hansel, C. (2011). SK2
623 channel expression and function in cerebellar Purkinje cells. *J Physiol J. Physiol. S*
624 *58914*: 3433–3440.

625 Jenkins, D.P., Strobaek, D., Hougaard, C., Jensen, M.L., Hummel, R., Sorensen, U.S., et
626 al. (2011). Negative gating modulation by (R)-N-(benzimidazol-2-yl)-1,2,3,4-
627 tetrahydro-1-naphthylamine (NS8593) depends on residues in the inner pore vestibule:
628 pharmacological evidence of deep-pore gating of K(Ca)₂ channels. *Mol.Pharmacol.* 79:
629 899–909.

630 Köhler, M., Hirschberg, B., Bond, C.T., Kinzie, J.M., Marrion, N. V, Maylie, J., et al.
631 (1996). Small-Conductance, Calcium-Activated Potassium Channels from Mammalian
632 Brain. *Science* (80-.). 273: 1709–1714.

633 Lam, J., Coleman, N., Lourdes A. Garing, A., and Wulff, H. (2013). The Therapeutic
634 Potential of Small-Conductance KCa₂ Channels in Neurodegenerative and Psychiatric
635 Diseases. *17*: 1203–1220.

636 Li, N., Timofeyev, V., Tuteja, D., Xu, D., Lu, L., Zhang, Q., et al. (2009). Ablation of a
637 Ca²⁺-activated K⁺ channel (SK2 channel) results in action potential prolongation in
638 atrial myocytes and atrial fibrillation. *J. Physiol.* 587: 1087–100.

639 Milkau, M., Köhler, R., and Wit, C. de (2010). Crucial importance of the endothelial K⁺
640 channel SK3 and connexin40 in arteriolar dilations during skeletal muscle contraction.
641 *FASEB J.* 24: 3572–3579.

642 Nardi, A., and Olesen, S.-P. (2008). BK channel modulators: a comprehensive
643 overview. *Curr. Med. Chem.* 15: 1126–46.

644 Nattel, S. (2002). New ideas about atrial fibrillation 50 years on. *Nature* 415: 219–26.

645 Pedarzani, P., McCutcheon, J.E., Rogge, G., Jensen, B.S., Christophersen, P.,
646 Hougaard, C., et al. (2005). Specific enhancement of SK channel activity selectively
647 potentiates the afterhyperpolarizing current IAHP and modulates the firing properties of
648 hippocampal pyramidal neurons. *J. Biol. Chem.* 280: 41404–41411.

649 Qi, X.Y., Diness, J.G., Brundel, B.J.J.M., Zhou, X.B., Naud, P., Wu, C.T., et al. (2014).
650 Role of small-conductance calcium-activated potassium channels in atrial
651 electrophysiology and fibrillation in the dog. *Circulation* 129: 430–440.

652 Schmitt, N., Grunnet, M., and Olesen, S.-P. (2014). Cardiac potassium channel
653 subtypes: new roles in repolarization and arrhythmia. *Physiol. Rev.* 94: 609–53.

654 Singh, H., Lu, R., Bopassa, J.C., Meredith, A.L., Stefani, E., and Toro, L. (2013).
655 mitoBKCa is encoded by the *Kcnma1* gene, and a splicing sequence defines its
656 mitochondrial location. *Proc. Natl. Acad. Sci. U. S. A.* 110: 10836–10841.

657 Skibsbye, L., Diness, J.G., Sørensen, U.S., Hansen, R.S., and Grunnet, M. (2011). The
658 duration of pacing-induced atrial fibrillation is reduced in vivo by inhibition of small
659 conductance Ca(2+)-activated K(+) channels. *J. Cardiovasc. Pharmacol.* 57: 672–681.

660 Southan, C., Sharman, J.L., Benson, H.E., Faccenda, E., Pawson, A.J., Alexander,
661 S.P.H., et al. (2016). The IUPHAR/BPS Guide to PHARMACOLOGY in 2016:
662 Towards curated quantitative interactions between 1300 protein targets and 6000
663 ligands. *Nucleic Acids Res.* 44: D1054–D1068.

664 Stocker, M., and Pedarzani, P. (2000). Differential distribution of three Ca(2+)-
665 activated K(+) channel subunits, SK1, SK2, and SK3, in the adult rat central nervous
666 system. *Mol. Cell. Neurosci.* 15: 476–493.

667 Strøbæk, D., Hougaard, C., Johansen, T.H., Sørensen, U.S., Nielsen, E.O., Nielsen,
668 K.S., et al. (2006). Inhibitory gating modulation of small conductance Ca²⁺-activated
669 K⁺ channels by the synthetic compound (R)-N-(benzimidazol-2-yl)-1,2,3,4-tetrahydro-
670 1-naphthylamine (NS8593) reduces afterhyperpolarizing current in hippocampal CA1
671 neurons. *Mol. Pharmacol.* 70: 1771–1782.

672 Strøbæk, D., Teuber, L., Jørgensen, T.D., Ahring, P.K., Kjær, K., Hansen, R.S., et al.
673 (2004). Activation of human IK and SK Ca²⁺-activated K⁺ channels by NS309 (6,7-
674 dichloro-1H-indole-2,3-dione 3-oxime). *Biochim. Biophys. Acta - Biomembr.* 1665: 1–
675 5.

676 Sørensen, U.S., Strøbæk, D., Christophersen, P., Hougaard, C., Jensen, M.L., Nielsen,
677 E., et al. (2008). Synthesis and structure-activity relationship studies of 2-(N-
678 substituted)-aminobenzimidazoles as potent negative gating modulators of small
679 conductance Ca²⁺-activated K⁺ channels. *J. Med. Chem.* *51*: 7625–7634.

680 Waks, J.W., and Zimetbaum, P. (2017). Antiarrhythmic Drug Therapy for Rhythm
681 Control in Atrial Fibrillation. *J. Cardiovasc. Pharmacol. Ther.* *22*: 3–19.

682 Wulff, H., Kolski-Andreaco, A., Sankaranarayanan, A., Sabatier, J.-M., and Shakkottai,
683 V. (2007). Modulators of small- and intermediate-conductance calcium-activated
684 potassium channels and their therapeutic indications. *Curr Med Chem* *14*: 1437–1457.

685 Zoni-Berisso, M., Lercari, F., Carazza, T., and Domenicucci, S. (2014). Epidemiology
686 of atrial fibrillation: European perspective. *Clin. Epidemiol.* *6*: 213.

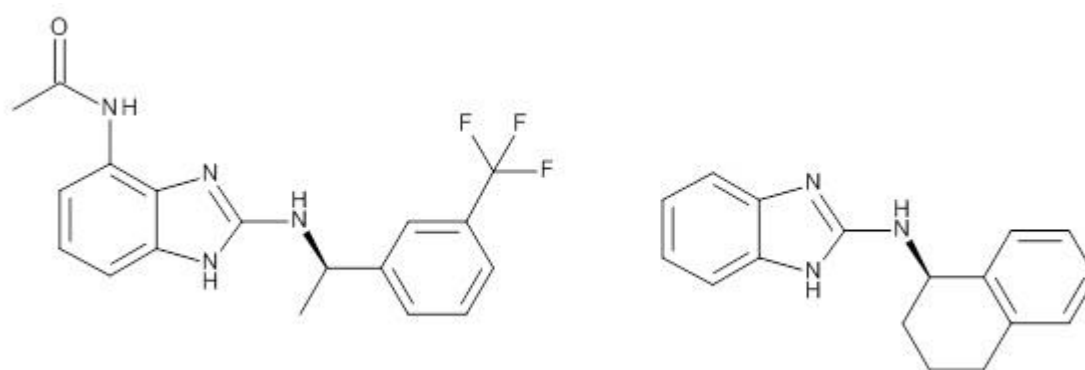
687

688 **Supporting information**

689 None supplied.

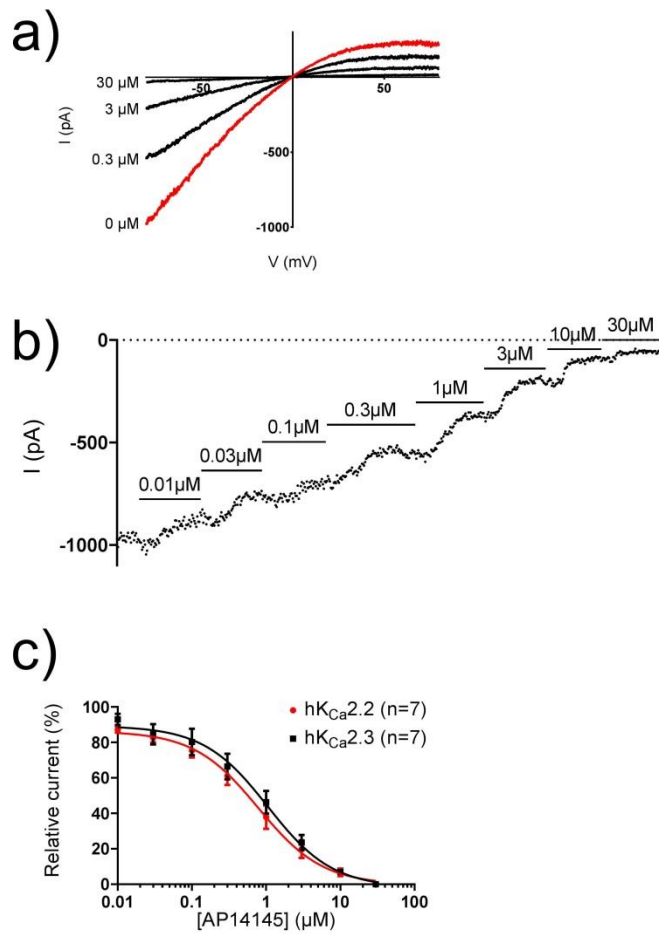
690

691 **Figures and figure legends**



692

693 Fig. 1. Chemical structures of AP14145 (left) and NS8593 (right).

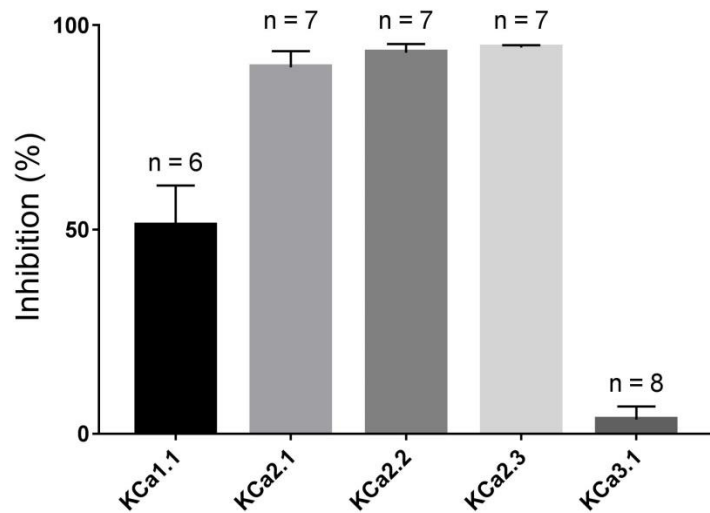


694

695 Fig. 2. a) Representative current-voltage recordings of the inhibition of hK_{Ca}2.3 by
 696 increasing concentrations of the drug AP14145 and b) its current-time plot obtained by
 697 inside-out patch clamp on HEK cells stably expressing the channel. c) Inhibition curves
 698 of AP14145 on both the hK_{Ca}2.2 (n = 7) and hK_{Ca}2.3 (n = 7) channel.

699

700

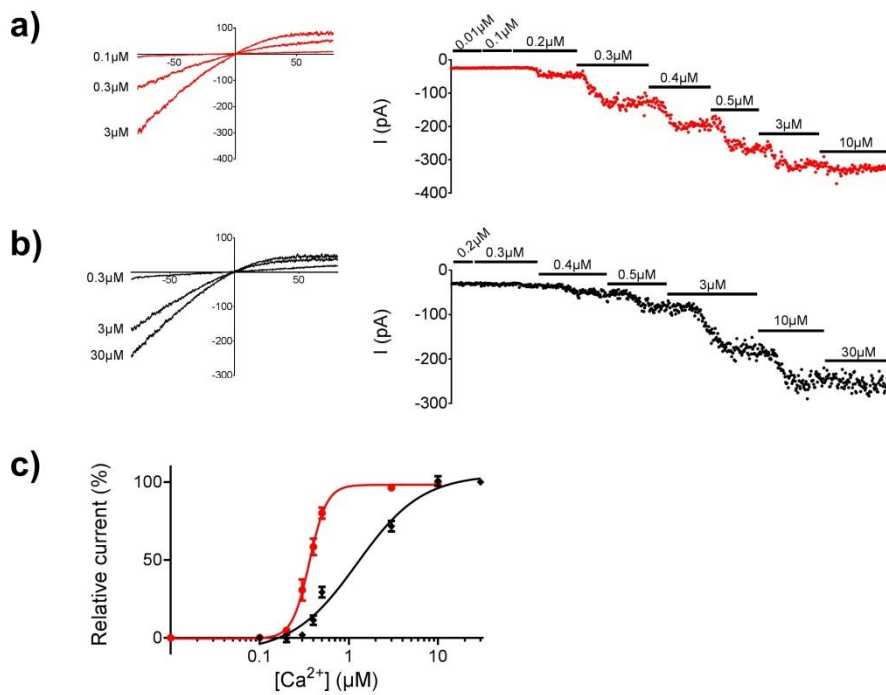


701

702 Fig. 3. Inhibitory effect of $10 \mu\text{M L}^{-1}$ AP14145 on $\text{KCa}1.1$, $\text{KCa}2.1$, $\text{KCa}2.2$, $\text{KCa}2.3$ and

703 $\text{KCa}3.1$ channels. All measurements were obtained by whole cell patch clamp except

704 $\text{KCa}2.2$, which were obtained by inside-out patch clamp.



705

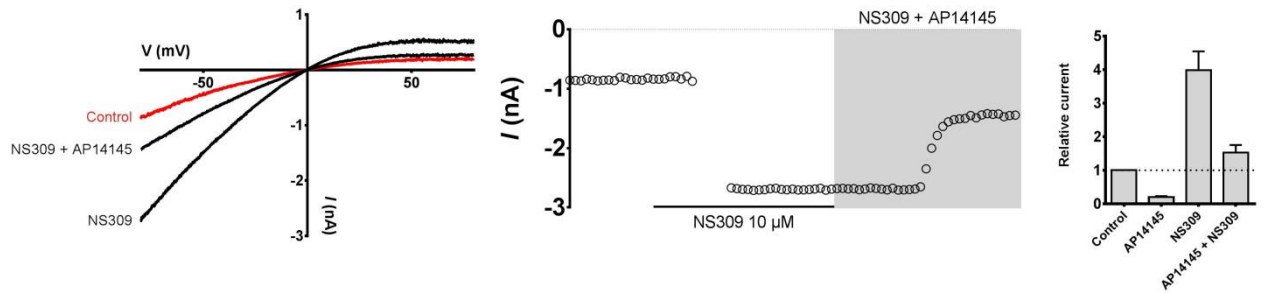
706 Fig. 4. Representative current-voltage plots (left) and their corresponding current-time

707 plots (right) of $\text{hKCa}2.3$ calcium activation a) in the absence of AP14145 and b) in the

708 presence of $10 \mu\text{M L}^{-1}$ AP14145. c) Calcium activation curves for the $\text{hKCa}2.3$ channel

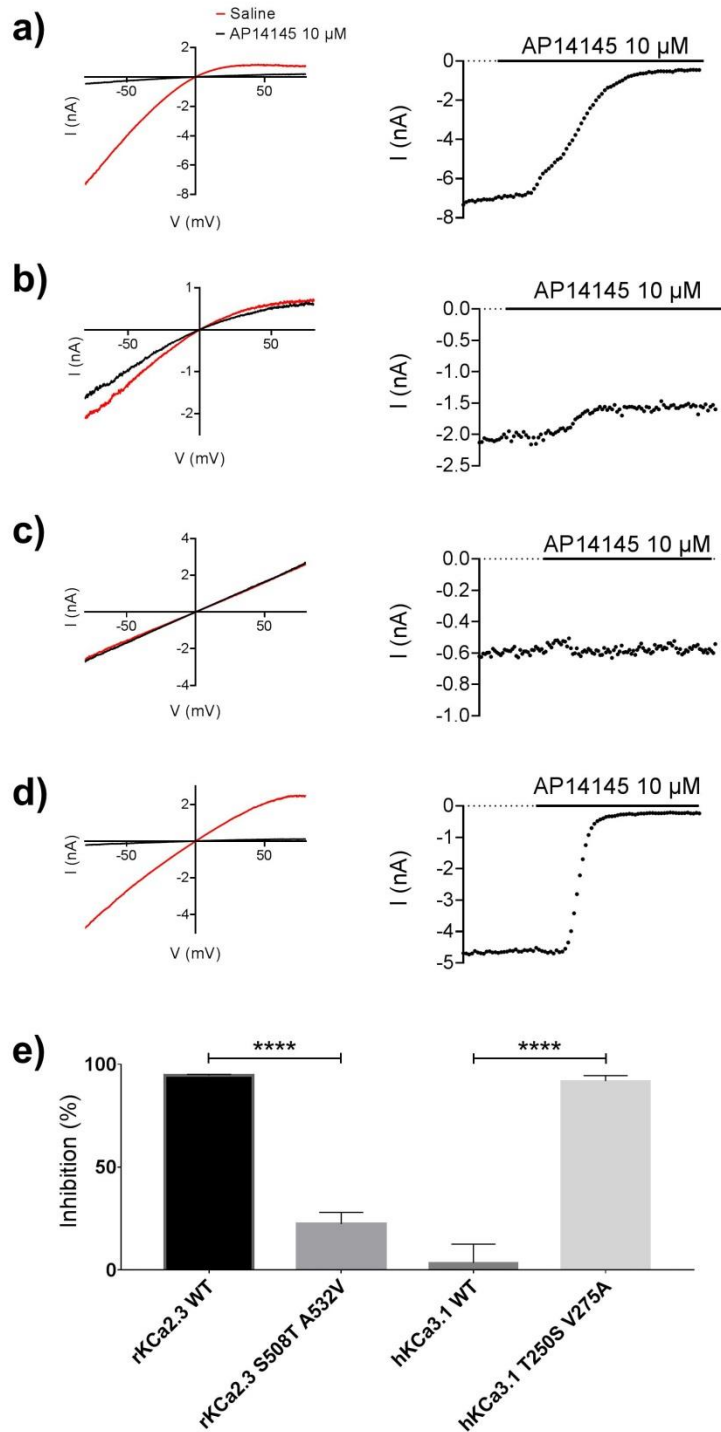
709 in the absence of AP14145 (red curve, $n = 9$) and in the presence of $10 \mu\text{M L}^{-1}$

710 AP14145 (black curve, $n = 7$).



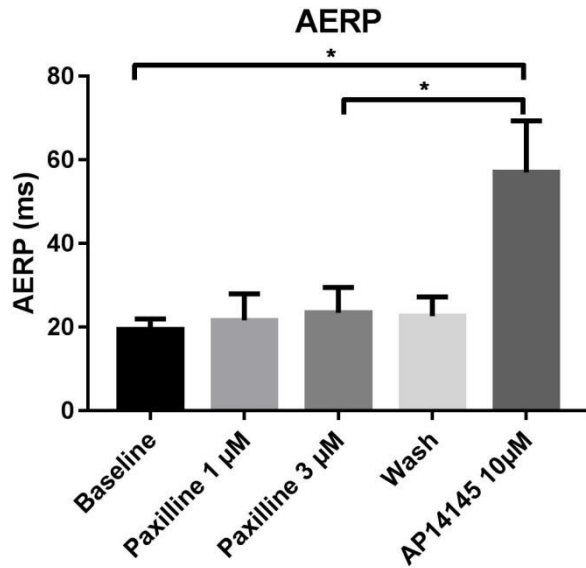
711

712 Fig. 5. Representative current-voltage plot (left) and its corresponding current-time plot
 713 (centre) of the effect of $10 \mu\text{M L}^{-1}$ NS309 in the absence and in the presence of $10 \mu\text{M}$
 714 L^{-1} AP14145 on excised $\text{hK}_{\text{Ca}2.3}$ patches. On the right, bar graph comparing the effects
 715 of $10 \mu\text{M L}^{-1}$ AP14145 ($n = 7$), $10 \mu\text{M L}^{-1}$ NS309 ($n = 7$), and $10 \mu\text{M L}^{-1}$ AP14145 + 10
 716 $\mu\text{M L}^{-1}$ NS309 ($n = 7$) on excised $\text{hK}_{\text{Ca}2.3}$ patches.



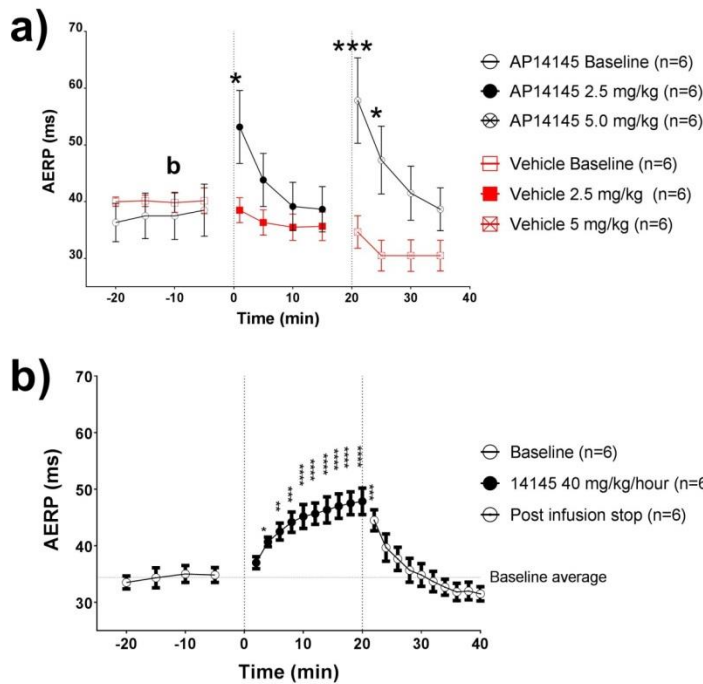
717

718 Fig. 6. Representative current-voltage plots (left) and current-time plots (right)
 719 depicting the effect of AP14145 $10 \mu\text{M L}^{-1}$ on HEK cells transiently transfected with a)
 720 rKCa_{2.3} WT, b) rKCa_{2.3} S508T A533V, c) hKCa_{3.1} WT and d) hKCa_{3.1} T250S V275A
 721 recorded using whole cell patch clamp. e) Bar graph comparing the inhibitory effect of
 722 $10 \mu\text{M L}^{-1}$ AP14145 on rKCa_{2.3} WT (n = 7), rKCa_{2.3} S508T A533V (n = 7), hKCa_{3.1}
 723 WT channel (n = 8) and hKCa_{3.1} T250S V275A (n = 7).



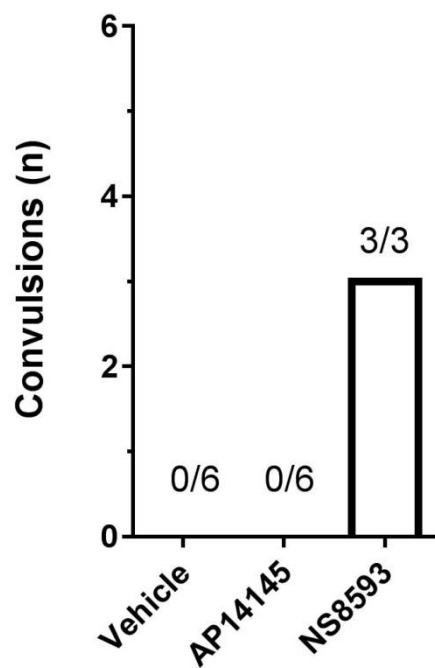
724

725 Fig 7. Effect of 1 $\mu\text{M L}^{-1}$ and 3 $\mu\text{M L}^{-1}$ of the $\text{K}_{\text{Ca}1.1}$ inhibitor paxilline and 10 $\mu\text{M L}^{-1}$
 726 AP14145 on the AERP of isolated perfused rat hearts (n = 5).



727

728 Fig. 8. Effects on AERP in closed chest in vivo rats: a) Bolus doses of 2.5 mg kg^{-1} and 5
 729 mg kg^{-1} AP14145 significantly increased the AERP compared to time matched controls
 730 receiving corresponding volumes of vehicle. b) AP14145 given as a constant rate
 731 infusion of 40 $\text{mg kg}^{-1} \text{h}^{-1}$ over 20 minutes increased AERP compared to the baseline
 732 average and returned towards baseline values post-infusion.



733

734 Fig. 9. Bar graph depicting the amount of convulsions triggered by the administration of
 735 the vehicle, 10 mg kg⁻¹ AP14145 and 10 mg kg⁻¹ NS8593.

736

737 Table 1. Calculated physicochemical properties and plasma protein binding (PPB) of
 738 NS8593 and AP14145.

	log D (pH 7.4)	log P	PSA (Å²)	PPB (% bound)
NS8593	4.0	4.1	41	95.38
AP14145	3.6	3.7	70	91.35

739

740

741